process are also given in the Figure. Because of the UMOST's concave structure,[5] it has a higher threshold voltage (V_T) and body effect coefficient than the NMOST fabricated on the same chip. An appropriate substrate bias (−0·5 V) results in an enhancement mode UMOST (V_T = 0·5 V) and a depletion mode NMOST (V_T = −1·2 V). The combination of the two devices can be used in an inverter configuration with a relative aspect ratio $(Z/L)_{UMOST}:(Z/L)_{NMOST}$ of 4 for low voltage (2·5 V) logic applications.[2] The resulting inverters are found to be capable of subpicojoule power-delay products in ring oscillator test structures and have a functional density of 250 gates/mm².

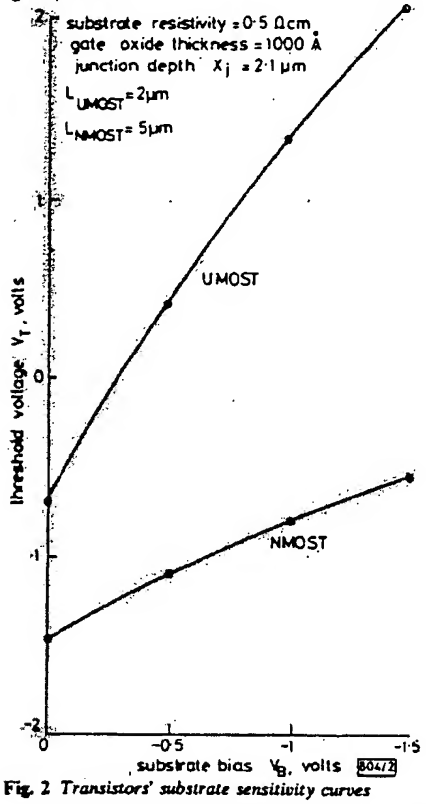

Fig. 2 *Transistors' substrate sensitivity curves*

This work was supported by the Natural Sciences & Engineering Research Council.

D. H. CHOI
C. A. T. SALAMA

Department of Electrical Engineering
University of Toronto
Toronto, Ontario, M5S 1A4, Canada

29th September 1981

References

1 DENNARD, R. H., GAENSSLEN, F. H., YU, H.-N., RIDEOUT, V. L., BASSOUS, E., and LEBLANC, A. R.: 'Design of ion-implanted MOSFET's with very small physical dimensions', *IEEE J. Solid-State Circuits*, 1974, SC-9, pp. 256–268

2 YU, H.-N., REISMAN, A., OSBURN, C. M., and CRITCHLOW, D. L.: '1 μm MOSFET VLSI technology: Part I—An overview', *IEEE Trans.*, 1979, ED-26, pp. 318–324

3 SALAMA, C. A. T.: 'A new short channel MOSFET structure (UMOST)', *Solid-State Electron.*, 1977, 20, pp. 1003–1009

4 HO, C. P., and PLUMMER, J. D.: 'Improved MOS device performance through the enhanced oxidation of heavily doped n^+ silicon', *IEEE Trans.*, 1979, ED-26, pp. 623–630

5 NATORI, K., SASAKI, I., and MASUOKA, F.: 'An analysis of the concave MOSFET', *ibid.*, 1978, ED-25, pp. 448–456

6 HESS, D. W., and DEAL, B. D.: 'Kinetics of the thermal oxidation of silicon in O_2/HCl mixtures', *J. Electrochem. Soc.*, 1977, 124, pp. 735–739

7 DEAL, B. D.: 'Thermal oxidation kinetics of silicon in pyrogenic H_2O and 5% HCl/H_2O mixtures', *ibid.*, 1978, 125, pp. 576–579

8 PASHLEY, R., KOKONNE, K., BOLEKY, E., JECMEN, R., LIU, S., and OWEN, W.: 'H-MOS scales traditional devices to higher performance levels', *Electronics*, 1977, 50, pp. 94–99

0013-5194/81/230879-02$1.50/0

ARRAYS OF CONCENTRIC RINGS AS FREQUENCY SELECTIVE SURFACES

Indexing terms: Antennas, Electromagnetic waves, Frequency selective surfaces, Dichroic mirrors

Concentric rings can be used as array elements in frequency selective surfaces. The transmission curves are more complex than those for simple rings, but provide more closely spaced reflection and transmission bands. In an example discussed here, a band centre frequency ratio of 1/1·3 is given by an array of compound elements with two concentric rings.

In a recent letter[1] we showed that simple rings used as array elements in frequency selective surfaces give reflection bands at least 25% in width with centre frequencies which are readily calculable, particularly when the elements are closely packed. Plots of the transmission coefficient against frequency are characterised by a fairly slow rise in transmission as the frequency decreases from resonance, giving a low-frequency transmission-band/reflection-band ratio of about 1:3. The transmission rises more rapidly with frequency above the reflection resonance but not sufficiently rapidly to ensure that grating lobe problems never arise in the upper transmission band. But by modifying the element to include additional concentric rings, it is possible to produce compound structures with modified transmission curves. Here we give some results for elements consisting of two concentric rings.

Fig. 1 shows the geometry of one of the arrays that we have studied. The elements were centred on a square lattice of side D = 4·7 mm. The outer radii of the rings were 1·5 and 2·2 mm with conductor widths of 0·35 and 0·2 mm, leaving a gap of 0·5 mm between the inner and outer rings. The arrays were again printed on a dielectric substrate of thickness 0·075 mm with ε_r = 2·33.

Fig. 2 compares the plane-wave transmission coefficients measured over the frequency range 8–40 GHz with values calculated for this surface using a modal analysis. As in Reference

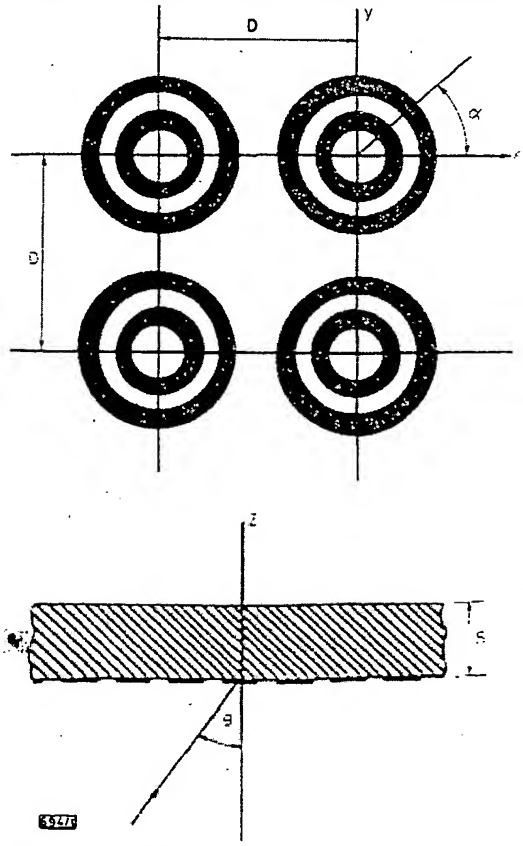

Fig. 1 *Array geometry*
E-field is incident in (y, z)-plane
θ = angle of incidence
s = thickness of dielectric substrate

i. currents ind
model as a se
two concentri

$$I = \sum_{k,m,j}$$

where m, n = i

The angle ϕ
point on the ci
a unit vector
curve in Fig.
used over the
magnetic field
modes were
$m_{max} = n_{max}$ =

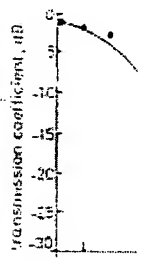

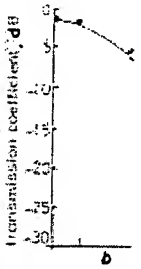

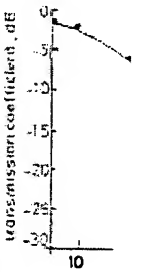

Fig. 2 *H-plane t*
– · calcu
expe
a θ = 0°
b θ = 30°
c θ = 45°

It can be see
between 4 and
GHz correspo
illustrated for
resonant frequ
incidence θ is
width of this
the reflection
normal incide
angles of inci
approximately
θ = 45°, the w
H-plane. In co
38 GHz is mu
ing in both pl
GHz at norma
not provide a

1, currents induced in the rings were expressed in the computer model as a series of sinusoidal or cosinusoidal modes. So for two concentric rings the element currents had the form

$$I = \sum_{k,m,n} (a_{km} \cos m\alpha + b_{kn} \sin n\alpha)\hat{\alpha} \quad (1)$$

where $m, n = 0, 1, 2, 3, \ldots$ and $k = 1, 2$.

The angle α defined on Fig. 1 expresses the position of a point on the circumference of either ring in the element and $\hat{\alpha}$ is a unit vector in the direction of increasing α. The computed curve in Fig. 2 was obtained when 49 Floquet modes[2] were used over the entire frequency range to express the electromagnetic fields close to the surface of the array. Five current modes were included for each ring in eqn. 1, i.e. $m_{max} = n_{max} = 2$.

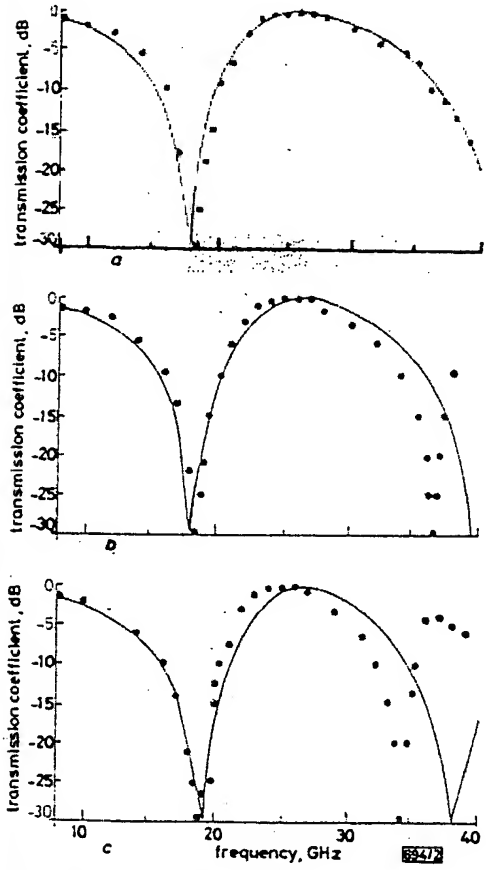

Fig. 2 *H-plane transmission coefficients*

· calculated values
●●● experimental results
a $\theta = 0°$
b $\theta = 30°$
c $\theta = 45°$

It can be seen that there are now two reflection resonances between 8 and 40 GHz. The low frequency resonance near 19 GHz corresponds to that observed for single-ring elements as illustrated for a triangular lattice in Fig. 1 of Reference 1. The resonant frequency is only marginally affected as the angle of incidence θ is varied from 0 to 45° in the principal planes. The width of this resonance, measured between the points where the reflection coefficient has fallen to −0·5 dB, is about 20% at normal incidence, but the reflection band that is common to all angles of incidence up to 45° in both planes has a width of approximately 13%. The narrowing occurs in the *E*-plane. At $\theta = 45°$, the width is only 13%, compared with 26% in the *H*-plane. In contrast, the location of the upper resonance near 38 GHz is much more sensitive to the angle of incidence, varying in both planes from about 35 GHz at $\theta = 45°$ to above 40 GHz at normal incidence. The upper resonance therefore does not provide a useful reflection band.

Fig. 2 shows that, at present, the computed and measured upper resonant frequencies are not in such good agreement as they are in the case of the lower resonance. Nevertheless, the behaviour of this resonance as the angle of incidence is changed is similar to that illustrated in Reference 1 for arrays of simple rings which are not close packed. The mean diameter/spacing ratio ($2r/D$) for our inner rings is about 0·56, while for the outer rings alone it is 0·89.

Although the upper resonant band itself may not be particularly useful, its presence modifies the shape of the transmission curve close to the lower resonance. The transmission coefficient rises more rapidly with frequency than it does in the case of simple close packed rings. Between the two resonances, there is a fairly narrow but significant band where the transmission loss is less than 0·5 dB. Its width common to all values of θ up to 45° is about 11% and its centre frequency is about 1·3 times that of the lower reflection band. Dichroic secondary mirrors incorporating arrays of compound rings therefore allow dual-band reflector antennas to be operated with significantly closer band spacing than can be attained with, for example, an array of crossed dipoles as the frequency selective surface. The band spacings are comparable with those obtained with waveguide dichroic mirrors,[3,4] or with arrays of Jerusalem crosses.[5,6] In a dual-band Cassegrain system with a dichroic secondary mirror, the feed design is simplified if the feed at the Cassegrain focus operates at the higher band. This would, of course, require the use of the Babinet complement of the array described here.

Acknowledgment: This work was supported by a research grant from the UK Science & Engineering Research Council.

E. A. PARKER
S. M. A. HAMDY
R. J. LANGLEY

The Electronics Laboratories
The University, Canterbury, Kent CT2 7NT, England

21st August 1981

References

1 PARKER, E. A., and HAMDY, S. M. A.: 'Rings as elements for frequency selective surfaces', *Electron. Lett.*, 1981, 17, (17), pp. 612–614
2 AMITAY, N., GALINDO, V., and WU, C. P.: 'Theory and analysis of phased array antennas' (Wiley, New York, 1972)
3 PARKER, E. A., LANGLEY, R. J., LANGSFORD, P. A., and DRINKWATER, A. J.: 'A reflector antenna with a dichroic Cassegrain mirror', *IEE Conf. Publ. 169*, 1978, pp. 70–74
4 LANGSFORD, P. A., and PARKER, E. A.: 'Cross polarisation of electromagnetic waves transmitted through waveguide dichroic plates', *IEE Proc. H, Microwaves, Opt. & Antennas*, 1981, 128, (1), pp. 1–5
5 LEONARD, T. W., and COFER, J. W.: 'A new equivalent circuit representation for the Jerusalem cross', *IEE Conf. Publ. 169*, 1978, pp. 65–69
6 LANGLEY, R. J., and DRINKWATER, A. J.: 'An improved empirical model for the Jerusalem cross', *IEE Proc. H, Microwaves, Opt. & Antennas* (to be published)

0013-5194/81/230880-02$1.50/0

EXTRACTION OF DECISION LEVEL FOR ENVELOPE-DETECTED AMPLITUDE-SHIFT KEYING

Indexing terms: Signal processing, Noise, Data transmission, Amplitude-shift keying

The optimum decision level for envelope-detected on/off amplitude-shift keying (ASK) in Gaussian noise is a complex function of the signal/noise ratio. A practical method is described which allows the decision threshold to be automatically extracted from the values at the decision instants of the binary levels.

Introduction: The solution for the optimum decision threshold for envelope-detected ASK in Gaussian noise is a well known